

Rapid Genome-wide Recruitment of RNA Polymerase II Drives Transcription, Splicing, and Translation Events during T Cell Responses

Kathrin Davari,^{1,2,5} Johannes Lichti,^{1,2,5} Christian Gallus,^{1,2} Franziska Greulich,¹ N. Henriette Uhlenhaut,¹ Matthias Heinig,³ Caroline C. Friedel,^{4,*} and Elke Glasmacher^{1,2,6,*}

¹Institute for Diabetes and Obesity (IDO), German Center for Environmental Health GmbH, Munich 85748, Germany

²German Center for Diabetes Research (DZD), German Center for Environmental Health GmbH, Munich 85764, Germany

³Institute for Computational Biology (ICB), German Center for Environmental Health GmbH, Munich 85764, Germany

⁴Institute for Informatics, Ludwig-Maximilians-Universität München, Munich 80333, Germany

⁵These authors contributed equally

⁶Lead Contact

*Correspondence: caroline.friedel@bio.ifi.lmu.de (C.C.F.), elke.glasmacher@helmholtz-muenchen.de (E.G.)
<http://dx.doi.org/10.1016/j.celrep.2017.03.069>

SUMMARY

Activation of immune cells results in rapid functional changes, but how such fast changes are accomplished remains enigmatic. By combining time courses of 4sU-seq, RNA-seq, ribosome profiling (RP), and RNA polymerase II (RNA Pol II) ChIP-seq during T cell activation, we illustrate genome-wide temporal dynamics for ~10,000 genes. This approach reveals not only immediate-early and post-transcriptionally regulated genes but also coupled changes in transcription and translation for >90% of genes. Recruitment, rather than release of paused RNA Pol II, primarily mediates transcriptional changes. This coincides with a genome-wide temporary slowdown in cotranscriptional splicing, even for polyadenylated mRNAs that are localized at the chromatin. Subsequent splicing optimization correlates with increasing Ser-2 phosphorylation of the RNA Pol II carboxy-terminal domain (CTD) and activation of the positive transcription elongation factor (pTEFb). Thus, rapid de novo recruitment of RNA Pol II dictates the course of events during T cell activation, particularly transcription, splicing, and consequently translation.

INTRODUCTION

In immune responses, extremely rapid and severe changes in gene expression and functional properties take place within activated cells of the immune system. For instance, ~800 genes are upregulated within 2–3 hr after macrophage activation, as demonstrated by genome-wide gene expression studies (Bhatt et al., 2012; Eichelbaum and Krijgsveld, 2014). Cells of the adaptive immune response, such as T helper cells, can be similarly activated and quickly reprogrammed in their gene expression

repertoire. Naive T helper cells differentiate from a quiescent state into different mature effector states (Zhu et al., 2010). Differentiation occurs in secondary lymphoid tissues through an interaction with dendritic cells presenting antigens, leading to clonal expansion of antigen-specific T cells (Murphy and Reiner, 2002). This process takes many hours, even up to 2 days, requiring cell division and changes in chromatin conformation (Agarwal and Rao, 1998). Mature T helper cells then become fully activated upon a second encounter with the antigen, after which they rapidly induce expression of various ligands and receptors, as well as extensive production of cytokines and chemokines. For instance, the pool of cytokines and receptors that define T helper 1 (Th1) cells consists of interferon γ (IFN γ), interleukin-2 (IL-2), tumor necrosis factor (TNF), CCR5, and CCR3 (Szabo et al., 2003; Wang et al., 2015). Their activation results in recruitment and activation of macrophages and B cells, leading to a systemic antigen-driven immune response (Asano et al., 1982). Classically, studies on gene regulation in the immune system are centered on epigenetic and transcriptional regulation (O'Shea, 2015; Singh, 2014; Smale, 2014). However, within the last few years, various studies revealed posttranscriptional mechanisms that control splicing, translation, and/or mRNA stability in immune cells (Anderson, 2008; Ansel, 2013; Carpenter et al., 2014; Piccirillo et al., 2014). Particularly in the context of Th1 effector cell activation, translational control mechanisms have been proposed to play a role in regulating cytokine production (Chang et al., 2013; Scheu et al., 2006). Despite this interest in these different gene regulatory programs, existing studies focus only on individual mechanisms and lack a global, dynamic, and comparative analysis among the different levels of regulation. Therefore, the global course of action during immune effector cell activation, ranging from transcriptional to posttranscriptional events, remains enigmatic.

To visualize the flow of transcriptional, as well as posttranscriptional regulation during Th1 effector cell activation, we performed a global time series experiment using 4-thiouridine sequencing (4sU-seq), total RNA sequencing (RNA-seq), and ribosome profiling (RP). 4sU-seq combined with total RNA-seq allows quantification of de novo transcription, turnover, and

splicing during defined intervals of cellular responses (Rutkowski et al., 2015; Windhager et al., 2012), while RP allows quantification of translational activity (Ingolia et al., 2012). We tracked real-time regulation for ~10,000 protein-coding genes, calculated translation and turnover rates, identified gene clusters that differed in speed and magnitude of regulation, and identified some genes that are posttranscriptionally regulated. However, transcription and translation were generally highly coupled, and distinct clusters mostly reflect differences in transcriptional regulation. Surprisingly, chromatin immunoprecipitation sequencing (ChIP-seq) with RNA polymerase II (RNA Pol II) revealed that for many genes, including immediate-early genes (IEGs), de novo recruitment of RNA Pol II, rather than release of paused RNA Pol II, promotes rapid upregulation. This recruitment of RNA Pol II coincides with a drop in global cotranscriptional splicing rates within the first hour of activation, even for transcripts that are already polyadenylated but remain at the chromatin. This is later overcome, correlating with an increased activation of the positive transcription elongation factor (pTEFb) a progressive shift from Ser-5 toward more Ser-2 phosphorylation of the carboxy-terminal domain (CTD) of RNA Pol II, and its increased binding to the cotranscriptional splicing factor U2AF65.

In summary, our study not only reveals the genome-wide course of events during a T helper response but also suggests a model in which rapid de novo recruitment of RNA Pol II dictates changes in transcription, which consequently lead to coupled changes in translation.

RESULTS

Genome-wide Real-Time Analysis Displays the Course of Events during a T Cell Response

To follow transcriptional and posttranscriptional regulation, we performed 4sU-seq, total RNA-seq, and RP in a time series experiment during Th1 effector cell activation. We activated fully differentiated Th1 cells and labeled them with 200 μ M 4-thiouridine (4sU) in 1 hr intervals (Figure 1A). Although 4sU labeling can influence cellular processes, such as rRNA synthesis (Burger et al., 2013), this experimental setup induced neither nuclear or cytoplasmic stress nor apoptosis, as tested for p53 or phospho-EIF2a in western blot analysis, respectively (Figure S1A–S1C) (Burger et al., 2013; Kedersha et al., 1999). We restricted the experiment to the first 4 hr of activation, because IFN γ levels decreased again after 4 hr (Figure S1D). A biological repeat of 4sU RNA, total RNA, and RP was performed for 0, 1, and 4 hr (Figure S1E), revealing similar read coverage and highly correlated expression values (quantified as FPKM [fragments per kilobase of exons per million mapped reads], rank correlation > 0.94) (Figure S1F). Analysis of changes in de novo transcription (using 4sU RNA) and translation (using RP) was performed for 9,420 protein-coding genes with FPKM > 1 for at least one time point in 4sU RNA, total RNA, and RP each (Table S1). In addition to standard normalization by numbers of mapped fragments, we performed normalization to ~3,400 housekeeping genes (Figure S2A) (Eisenberg and Levanon, 2013). Before this additional normalization, median fold changes of housekeeping genes varied slightly across time points without any consistent

trend toward either up- or downregulation (Figure S2A). Thus, we considered these variations experimental artifacts and corrected for them.

This experimental setup allows a comparative analysis of regulation in speed and magnitude on the level of transcription and translation for ~10,000 genes during the Th1 cell response (Figure 1B). Most of the top upregulated genes after 1 hr of activation were initiators of the immune response, inflammatory cytokines, and chemokines (e.g., *Ifn γ* , *Il2*, *Il3*, *Tnf*, and *Ccl4*) (Figure 1C), but they also included some negative regulators of the immune response, such as *Bcl3* and *Socs* family members (Figure S2B; Table S2).

Hierarchical cluster analysis for upregulated genes (1,185 genes > 2-fold upregulated until 4 hr in at least two consecutive time points) based on fold changes in de novo transcription (4sU RNA) and translation (RP) at 1, 2, and 4 hr (Figure S2C) identified gene-specific differences in upregulation. The six largest clusters, representing ~95% of upregulated genes, are shown in Figure 1D. Essentially, we observed three distinct types of behavior: (1) an immediate-early response, marked by a sharp increase in expression followed by a decrease or plateau (clusters 3 and 5); (2) a secondary response, marked by a more gradual increase in expression and varying delays between de novo transcription and translation (clusters 1, 2, and 4); and (3) a group of genes with mild transcriptional regulation but some translational upregulation (cluster 6). Example genes for each cluster are illustrated in Figure 1E. Cluster 5 contains several immunological genes, such as *Ifn γ* , *Fos*, *JunB*, and *Il3*, that have been previously suggested as immediate-early genes (IEGs). We thus hypothesize that cluster 5 genes generally represent IEGs, many of which have not been studied in the context of a T cell response so far, e.g., *Nedd9* and *Spin1*. Functional enrichment analysis for all clusters (Figure 1F; Table S3) (Huang et al., 2009) identified cytokine activity as significantly associated with cluster 5 but also with cluster 2 (containing, e.g., *Il2* and *Irf4*). Cluster 3, which also represented an immediate-early response, likewise contained a number of immunologically important genes, such as *Traf1/4*, *Irf8*, or *Batf*, but was only functionally enriched for receptor proteins.

Hierarchical clustering was also performed for 1,574 downregulated genes (Table S4). We confirmed downregulation for exemplary genes with qRT-PCR after spiking in GFP plasmids that remained episomal (Figure S2D). Cluster analysis identified four major clusters, with most genes (~78%) belonging to cluster 1 (Figure S2E). We again observed three types of behaviors: (1) an early response in de novo transcription (cluster 3), (2) a continuous downregulation on the transcriptional and translational levels (cluster 1), and (3) a mild downregulation on the transcriptional level but some translational regulation (cluster 2 and 4) (Figure S2F). Some interesting genes are highlighted that have not been studied in the context of T cell effector function, e.g., some transcription factors, RNases, and CCCH-type Zinc finger genes (Figure S2G).

Global Coupling of Transcriptional and Translational Regulation

To further investigate the extent of posttranscriptional regulation, we first compared global translation rates (FPKM in RP versus

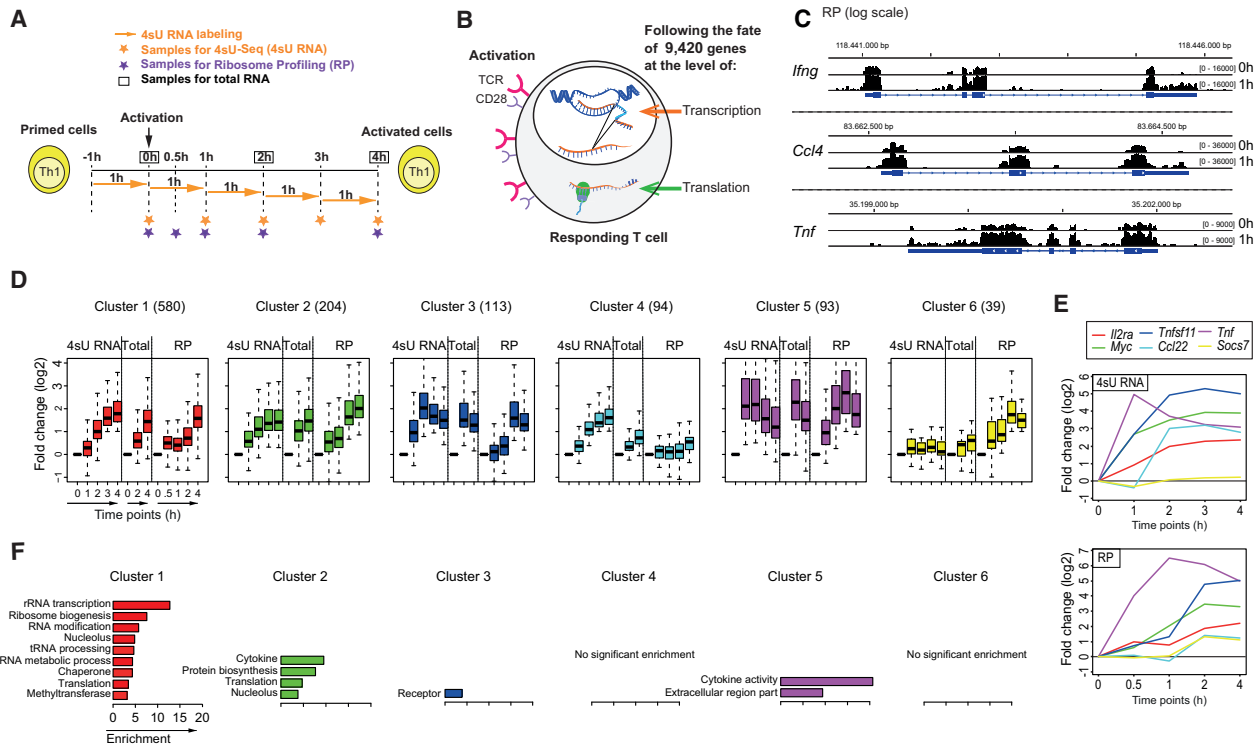


Figure 1. Gene Responses Differ in Speed and Magnitude on the Transcriptional and Translational Levels

(A) Experimental setup. Th1 cells were activated at $t = 0$ hr with anti-CD3 and anti-CD28 antibodies. 4sU labeling in 1 hr intervals (indicated by orange arrows), followed by sequencing (4sU-seq; orange asterisks), was performed during the first 4 hr of activation. RP (purple asterisks) and sequencing of total RNA (black boxes) were performed at indicated time points.

(B) Model shows the level of gene regulation in activated T cells that can be analyzed with the experimental setup explained in (A).

(C) Mapped RP reads (log scale) for *lfnlg*, *Ccl4*, and *Tnf* at 0 and 1 hr after activation. Gene annotation is indicated below, with exons depicted as boxes (smaller boxes are untranslated regions) and introns depicted as lines. For each time point, the range of read counts (y axis) is shown in square brackets.

(D) Hierarchical clustering of all upregulated genes based on log₂ fold changes in de novo transcription (4sU RNA) and translation (RP) at 1, 2, and 4 hr upon activation. Boxplots illustrating the distribution of log₂ fold changes for the six largest clusters are shown, and the number of genes in each cluster is indicated in brackets.

(E) Fold changes over time of representative genes for each cluster. Colors are the same as for the respective cluster in (D).

(F) Enriched gene ontology (GO) terms ($p < 0.001$) and protein keywords (from SwissProt and Protein Information Resource [PIR]) for the functional enrichment analysis performed with DAVID are shown for each cluster, ordered according to their enrichment value. Redundant terms were removed with DAVID's clustering option.

FPKM in total RNA) between time points (Table S1). Although genes varied considerably in translation rates, e.g., *Sike1*, *Gata3*, *Actb*, and *lfnlg* (Figure 2A) and we observed a slight shift at 1 hr in replicate 2 (Figure S3A), there was no evidence for global changes in translation rates at any other time (Figures 2B and S3B). This included *lfnlg*, for which translation rates hardly changed (Figure S3C). Furthermore, 4sU RNA and RP, as well as total RNA and RP, were highly correlated across the time course for *lfnlg* (>0.89 and >0.96 , respectively). FPKM values from sequencing were confirmed by quantifying *lfnlg* mRNA levels with qRT-PCR and IFN γ protein levels with intracellular fluorescence-activated cell sorting (FACS) staining (Figure S3D). Other major cytokines seemed to be similarly upregulated in a coupled manner (Figure S3E).

A global correlation analysis of fold changes in 4sU RNA, total RNA, and RP compared to non-activated cells showed a similar trend (Figure 2C). Four hours after activation, fold changes in translation were highly correlated to fold changes in both total

RNA (correlation 0.88) and de novo transcription (correlation 0.85). Correlation tended to be higher among different types of measurements (4sU RNA, total RNA, or RP) at the same time point than for the same type of measurement at different time points. Here, fold changes in total RNA tended to be smaller than fold changes in 4sU RNA (Figure 2D), which might be explained by differences in RNA turnover, because changes in de novo transcription take longer to measurably affect total RNA levels, particularly if basal RNA turnover is low (Friedel et al., 2009). We quantified RNA turnover in non-activated cells and correlated this to ratios in fold changes of newly transcribed RNA to total RNA at 4 hr (Figure 2E), which showed a strong negative correlation (-0.58). In particular, genes with low turnover ($<5\%$) displayed higher fold changes (>2 -fold) in newly transcribed RNA than in total RNA. Turnover rates for all regulated genes can be found in Table S1, and representative examples are displayed in Figure 2F.

Analysis of turnover rates for our previously defined up- and downregulated clusters found that upregulated clusters 3

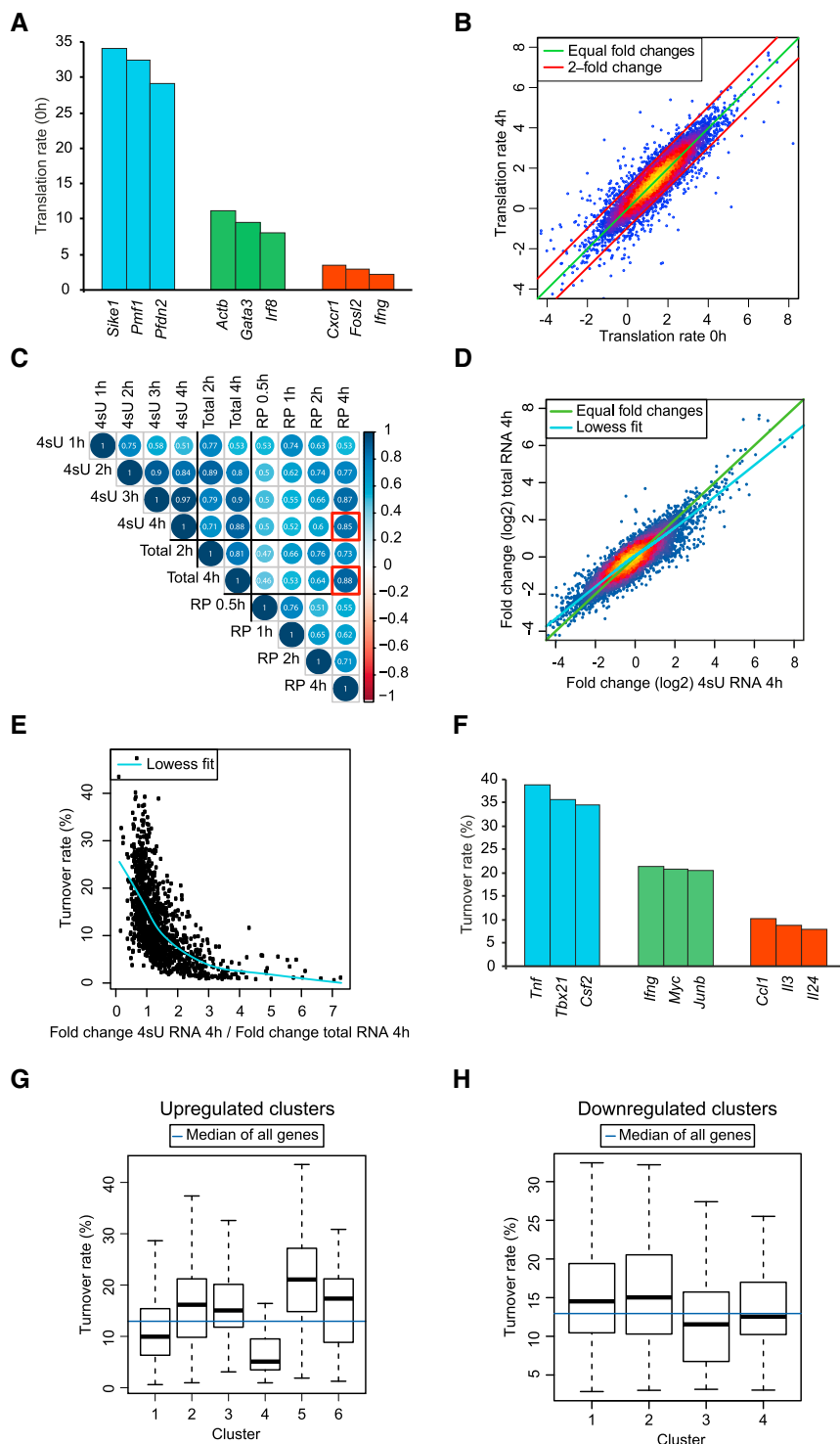


Figure 2. Transcriptional Regulation Dictates the Gene Response

(A) Translation rates for selected genes at 0 hr. (B) Scatterplot comparing translation rates between non-activated and activated (at 4 hr) Th1 cells (green line, equal fold changes; red line, 2-fold changes). (C) Global correlation analysis of fold changes among all samples at all time points of newly transcribed (4sU), total, and translated RNA (RP) for 9,420 protein-coding genes. Rank correlation is indicated for each time point. The high correlation at 4 hr between translated (RP) and total or 4sU RNA, respectively, is highlighted with red boxes. (D) Scatterplot comparing fold changes at 4 hr in 4sU RNA versus total RNA. Local regression fit using locally weighted scatterplot smoothing (LOWESS) and equal fold changes are indicated by cyan and green lines, respectively. (E) Scatterplot of RNA turnover rates against the fold change observed in 4sU RNA at 4 hr compared to the fold change in total RNA at the same time point (cyan line, local regression fit estimated using LOWESS). (F) RNA turnover rates for selected genes. (G and H) Distributions of RNA turnover rates for each cluster of upregulated (G) and downregulated (H) genes are represented as boxplots (horizontal blue line, median RNA turnover rate over all genes).

and 5 with high coupling among 4sU RNA, total RNA, and translation showed significantly higher basal turnover (Figure 2G). Similarly, differences between downregulated clusters 1 and 3 (Figure 2H) may be explained by differences in basal turnover. For upregulated cluster 6 and downregulated clusters 2 and 4,

translation outpaces alterations in both 4sU RNA and total RNA levels, suggesting translational regulation of these 219 genes during activation. Previously, regulation of translational activity has been described in the context of T cell activation by mechanistic target of rapamycin (mTOR) signaling-mediated phosphorylation of 4E-BP1 (Hamilton et al., 2014). We confirmed strong phosphorylation of 4E-BP1, suggesting that the shift in translation rates at 1 hr might reflect mTOR activation (Figures S3A and S3F). Nevertheless, our data indicate that most (>92%) changes in translation during the actual response are determined by changes in total mRNA levels, which mostly follow alterations in 4sU RNA with a delay depending on basal RNA turnover rates.

Rapid Recruitment of RNA Pol II Mediates Transcriptional Upregulation

Factors involved in the process of translation and protein folding were systematically upregulated in transcription. Here, ~48% of genes with a function in translation were upregulated in de novo transcription and translation (Figure S4A), and related functions were enriched in upregulated cluster 1 (Figure 1F). In contrast, genes annotated with transcriptional processes were not generally upregulated

(Figures S4A and S4B). Because many transcription factors have already been described with a function in T cells (O'Shea, 2015), we applied EnrichR (Chen et al., 2013) to identify transcription factors with targets enriched among upregulated clusters (Figure 3A). This identified c-Myc as key regulator in clusters 1, 2, and 4 and STAT3, STAT4, and RelA as key regulators of clusters 3 and 5. A subsequent analysis of c-Myc binding sites determined with ChIP-seq in CD8⁺ T cells (Chou et al., 2014) confirmed that c-Myc binding sites are enriched among upregulated genes in general (Figure S4C) and genes from upregulated clusters 1, 2, and 4 in particular (Figure S4D).

Because these transcription factors act immediately after activation and are not upregulated themselves (except c-Myc) (Figure S4E), we wondered whether this holds true for the transcription machinery and includes a “ready to go” RNA Pol II. Stalling and subsequent release of RNA Pol II has been described as an important mechanism for rapid cellular activation processes (Core et al., 2008; Muse et al., 2007). We therefore performed ChIP-seq of RNA Pol II at 0, 0.5, and 2 hr in two replicates, identifying on average >9,400 peaks for >5,600 genes (see Table S5 for identified peaks and their location relative to annotated genes). Peaks were clearly centered on the transcription start site (TSS) of genes, indicating the presence of paused RNA Pol II molecules (Figure S4F). Figure 3B illustrates the distribution of ChIP-seq reads across the gene body for *Irfng* (Figure S4G for replicate 2), which suggests some paused RNA Pol II at the TSS at 0 hr, followed by rapid intensification of the RNA Pol II signal and movement into the gene body in activated cells.

Presence of RNA Pol II at the promoter (TSS \pm 500 nt) was quantified for genes analogous to the FPKM value for RNA-seq. This showed a positive correlation between the abundance of RNA Pol II on the promoter to de novo transcription (Figures S4H and S4I), and fold changes in promoter RNA Pol II abundance, particularly between 0 and 2 hr, correlated well with fold changes in de novo transcription (Figures 3C and S4J for replicate 2). Thus, upregulation of genes coincides with increased abundance of RNA Pol II at the promoter, particularly for the identified IEGs in upregulated cluster 5 (Figure 3D). For many of these IEGs, RNA Pol II peaks were hardly detectable at 0 hr. Specifically, for 8 of 14 genes that were >50-fold upregulated within the first hour, RNA Pol II peaks were identified at the promoter for the first time at 30 min or later (e.g., *Egr2*, *Egr3*, and *Tnfrsf14* in Figure 3E and *Ii3* in Figure S4K). Most of these genes were not or were only lowly expressed at 0 hr. Other IEGs with some de novo transcription in non-activated cells, such as *Fosl2*, *Ii10*, and *Tnf* had a significant RNA Pol II peak at 0 hr but also experienced a massive increase in the RNA Pol II signal at the promoter at 0.5 hr that indicates de novo recruitment (Figure 3F).

To investigate to which extent release of paused RNA Pol II contributes to the massive and rapid upregulation of many genes, we calculated the change over time in promoter-to-gene body ratio of the RNA Pol II (FPKM at the promoter to FPKM on the gene body). Although for *Irfng* this ratio was reduced by around 50% at 30 min, there was no general correlation between changes in the RNA Pol II promoter-to-gene body ratio and fold changes in de novo transcription (Figure 3G). We iden-

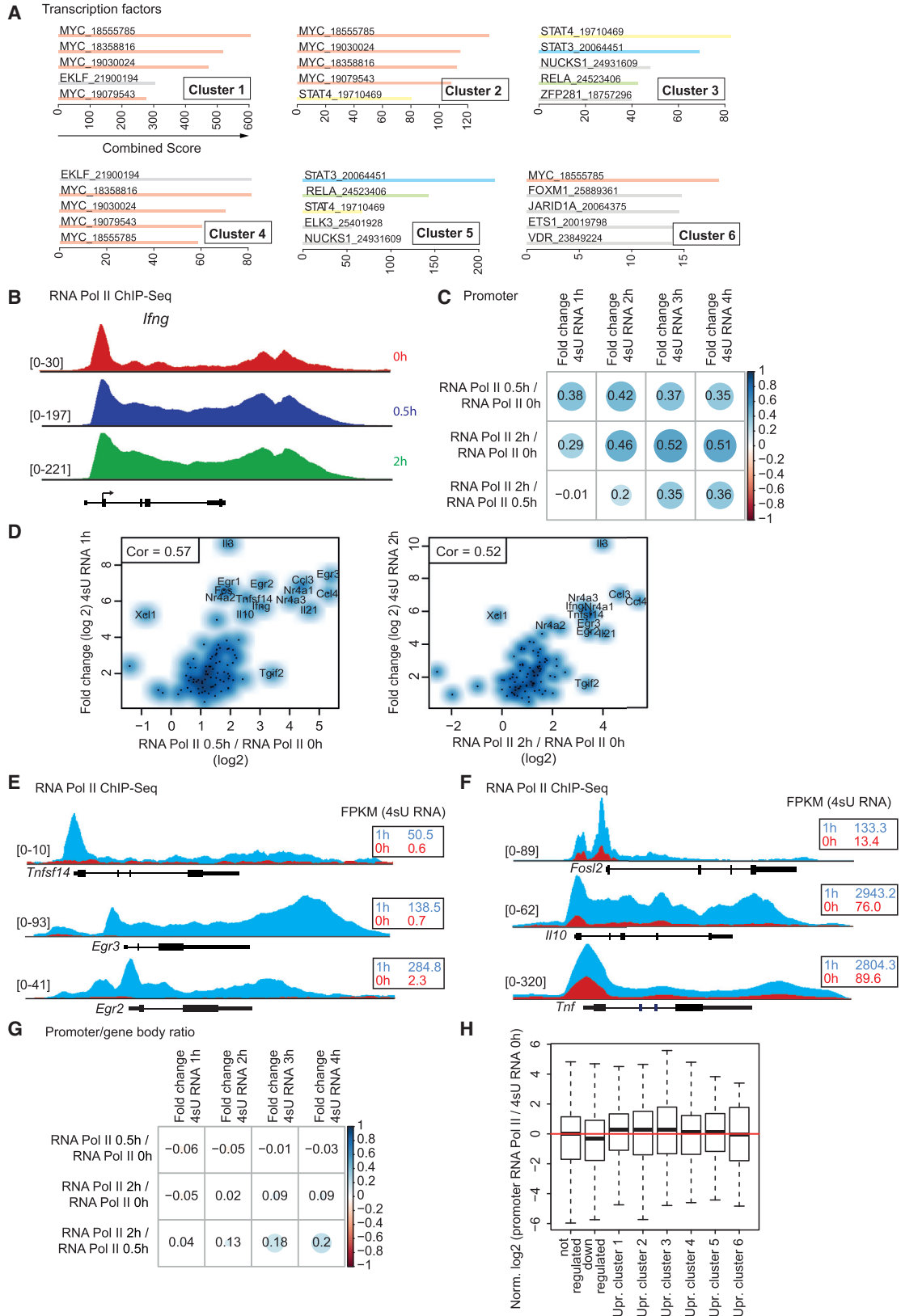
tified only 29 genes with significant RNA Pol II abundance at the promoter at 0 hr (FPKM > 1), a >2-fold change in 4sU RNA at 4 hr, and at least a 30% reduction in promoter-to-gene body ratio of RNA Pol II during activation (Figure S4L).

Finally, we evaluated whether rapidly upregulated genes appeared to be more primed for upregulation by increased presence of RNA Pol II at the promoter before activation. For this purpose, we divided promoter RNA Pol II abundance at 0 hr by the level of de novo transcription at 0 hr and compared this ratio among non-regulated genes, downregulated genes, and clusters of upregulated genes (Figure 3H). Normalized to non-regulated genes, the RNA Pol II/4sU RNA ratio at 0 hr of upregulated clusters 1–5 was increased on average by 4%–23%. Furthermore, downregulated genes had 20% lower RNA Pol II/4sU RNA ratios on average. However, overall correlation between the RNA Pol II/4sU RNA ratio and the fold changes in 4sU-RNA was very weak (≤ 0.1); in particular, it was weaker than the correlation between promoter RNA Pol II fold changes and 4sU RNA fold changes. Thus, although release of paused RNA Pol II may play a role in T cell activation, rapid de novo recruitment of RNA Pol II, particularly for IEGs, is the dominant mechanism to ensure rapid transcriptional upregulation during a T cell response.

Reduction of Cotranscriptional Splicing Rates Early after Activation

The rapid de novo recruitment of RNA Pol II made us speculate whether related processes are affected, such as cotranscriptional splicing, which is linked to activation states of RNA Pol II (Bentley, 2014). When looking at mapped reads for *Ii2*, we saw that the relative frequency of intronic reads increased 1 hr after activation but later decreased (Figure 4A). Surprisingly, IFN γ did not appear to undergo such an initial drop in splicing (Figure S5A). To investigate whether IFN γ really is unaffected, we additionally performed 30 min 4sU labeling for non-activated cells and the first 30 min of activation. This allowed quantification of changes in splicing rates within the first 30 min of activation and showed that splicing rates for *Irfng* dropped at this time (Figure S5B).

We then quantified the fraction of fully spliced transcripts for each gene and grouped genes into five categories: (1) genes >4-fold downregulated at 1 hr, (2) genes >4-fold downregulated at 4 hr but not at 1 hr, (3) genes not regulated at 4 hr, (4) genes upregulated early at 1 hr, and (5) genes upregulated late at 4 hr. Astonishingly, this showed a general trend for all expressed genes, with an initial drop followed by a gradual optimization of splicing rates beyond levels in non-activated cells (Figure 4B, confirmed by the biological replicate in Figure S5C). Fluctuations were more pronounced for early upregulated genes, explaining the observed difference between *Ii2* and IFN γ . Because >4-fold downregulated genes also experience the drop in splicing rates and we observe a drop in total RNA synthesis at the beginning of activation that is not due to rRNA (Figures S5D and S5E), this drop in splicing rates does not simply reflect an overall increase in nascent transcript production at the beginning of activation. Furthermore, splicing factors were neither regulated on the transcriptional or translational level nor noticeably altered in protein levels (Figures S5F and S5G).



(legend on next page)

Reduction in splicing rates has previously been described in macrophage activation, in which transcripts in the chromatin fraction were found to be incompletely spliced, despite already being polyadenylated (Bhatt et al., 2012). We thus isolated RNA from the whole nucleus and performed qRT-PCR for polyadenylated mRNAs with primers identifying either spliced or unspliced transcripts for three highly expressed and regulated genes (*Irfng*, *Irf3*, and *Ccl3*) (Figure 4C). This showed a clear shift in the spliced/unspliced ratio for nuclear polyadenylated RNA (Figures 4D and S5H), with ratios dropping at 30 min and then increasing. The same was observed for polyadenylated RNA obtained by further fractionating chromatin from nucleoplasm (Figures 4E and S5).

Phosphorylation States of the CTD of RNA Pol II Correlate with Fluctuations in Splicing Rates

Cotranscriptional splicing has been linked to certain epigenetic states, particularly H3K36me3 marks (Haque and Oberdoerffer, 2014; Schwartz et al., 2009) and phosphorylation states of the RNA Pol II CTD (Bentley, 2014; Phatnani and Greenleaf, 2006). We thus also performed H3K36me3 ChIP-seq at 0, 0.5, and 2 hr of activation. This showed that H3K36me3 is enriched over gene bodies (Figures S5J and S5K) and that it marks expressed genes (Figures S5L and S5M). Furthermore, for a few genes, such as *Irfng*, *Junb*, and *Fos*, we observed either a shift of reads at 2 hr toward the 5' end of genes or an increase in abundance (Figure S5N), which has previously been described to be related to cotranscriptional splicing (Schwartz et al., 2009; Venkatesh and Workman, 2013). However, at 0.5 hr, when the global drop in splicing was most prominent, there was either only an intermediate shift (as for *Fos*) (Figure S5N) or no shift toward either the 5' or the 3' end. Furthermore, the relative enrichment of H3K36me3 on exons did not significantly change on a global level at any time point for non-, down-, or upregulated genes (Figure S5O). Thus, changes in H3K36me3 marks did not explain the observed global drop in splicing.

Subsequently, we focused on changes in the phosphorylation states of RNA Pol II. Both our 4sU RNA and RP data showed no change in RNA Pol II subunit expression (Figure 5A). In contrast, unique RNA Pol III subunits, transcribing, e.g., 5S rRNA, are upregulated in line with the general upregulation of translational

genes (Figure S4A). We then performed western blot analysis with the anti-RPB1 antibody, which recognizes unmodified RNA Pol II but also hyper-phosphorylated CTD (Figure 5B) (Schüller et al., 2016). This showed a massive switch to the hyper-phosphorylated form after 2 hr, correlating with the time at which splicing rates are optimized. Because this antibody preferentially recognizes Ser-2 hyper-phosphorylation of the CTD, we also used antibodies differentiating between Ser-5 (indicating transcription initiation) and Ser-2 (indicating elongation) phosphorylation (Listerman et al., 2006; Schüller et al., 2016). This showed a substantial increase in Ser-5 phosphorylation of the CTD at the beginning of activation (Figure 5C). In contrast, Ser-2 phosphorylation increased gradually until 2 hr, when it became the dominant modification. Ser-5 phosphorylation of RNA Pol II is found predominantly near the TSS, whereas Ser-2 phosphorylation of RNA Pol II is enriched toward the 3' end of genes (Komamitsky et al., 2000). Consistent with this, changes in splicing rates in our data were most noticeable close to the TSS (Figures 5D and 5E). Furthermore, immunoprecipitation of U2AF65, a well-known cotranscriptional splicing factor that interacts with Ser-2 phosphorylated CTD (Listerman et al., 2006), showed an increased interaction after activation (Figure 5F). Ser-2 phosphorylation is mediated by activated pTEFb, consisting of cyclin T1 and cyclin-dependent kinase 9 (CDK9), which is activated by phosphorylation of CDK9 (Baumli et al., 2008; Jonkers and Lis, 2015). We thus tested activation of pTEFb by immunoprecipitating for cyclin T1. Using antibodies that recognize either total or phosphorylated CDK9, we found that its longer isoform was massively phosphorylated within the complex no later than 2 hr after activation (Figure 5G). This demonstrates activation of pTEFb, which likely facilitates Ser-2 phosphorylation of the RNA Pol II CTD in T cells.

DISCUSSION

We present the first comprehensive analysis on real-time temporal dynamics of transcription, splicing, and translation during T effector cell activation. Our data suggest a model in which T cells massively change their functional program by regulation of >2,000 genes. Here, changes in transcription and translation are extremely coupled for >90% of genes, and only a few genes

Figure 3. On-Time Recruitment of RNA Pol II Mediates Rapid Changes in Transcription

- (A) Enrichment analysis with EnrichR (Chen et al., 2013) for transcription factor targets identified experimentally using ChIP-seq or ChIP-chip for each upregulated cluster. Bars indicate the combined score determined by EnrichR (calculated from the p value and a rank-based score) and are annotated with both the transcription factor and the PubMed identifier (ID) for the corresponding publication. Results are shown for the top datasets with $p < 0.001$ (at most ten).
- (B) Mapped sequencing reads (RNA Pol II ChIP-seq) for *Irfng* for non-activated, 0.5 hr activated, and 2 hr activated Th1 cells. Gene annotation is indicated as in Figure 1C. The range of read counts (y axis) is shown in square brackets.
- (C) Rank correlation between fold changes in promoter RNA Pol II abundance between each pair of time points and fold changes in 4sU RNA compared to non-activated cells.
- (D) Scatterplot comparing \log_2 fold changes in promoter RNA Pol II abundance at 0.5 and 2 hr to \log_2 fold changes in 4sU RNA at 1 and 2 hr and to non-activated cells for genes of upregulated cluster 5. Rank correlation is indicated.
- (E and F) Mapped sequencing reads (RNA Pol II ChIP-seq) for selected genes at 0 hr (red) and 0.5 hr (light blue) after activation. Samples in (E) do not show significant peaks in non-activated cells, whereas (F) shows examples with significant peaks in non-activated samples. For comparison purposes, 4sU RNA FPKM values are indicated in the black box. The range of read counts (y axis) is depicted in brackets. Gene annotation is indicated as in Figure 1C.
- (G) Rank correlation between fold changes in promoter-to-gene body ratio for RNA Pol II compared to fold changes in 4sU RNA at all time points.
- (H) Ratios of RNA Pol II abundance to 4sU RNA at 0 hr were calculated for non-regulated genes, downregulated genes, and genes of the six major upregulated clusters. Ratios were normalized by dividing by the median ratio for non-regulated genes, and distribution of normalized ratios for each group are illustrated using boxplots. Positive values thus indicate more RNA Pol II at the promoter than expected from baseline de novo transcription at 0 hr compared to non-regulated genes (red horizontal line, median value for non-regulated genes).

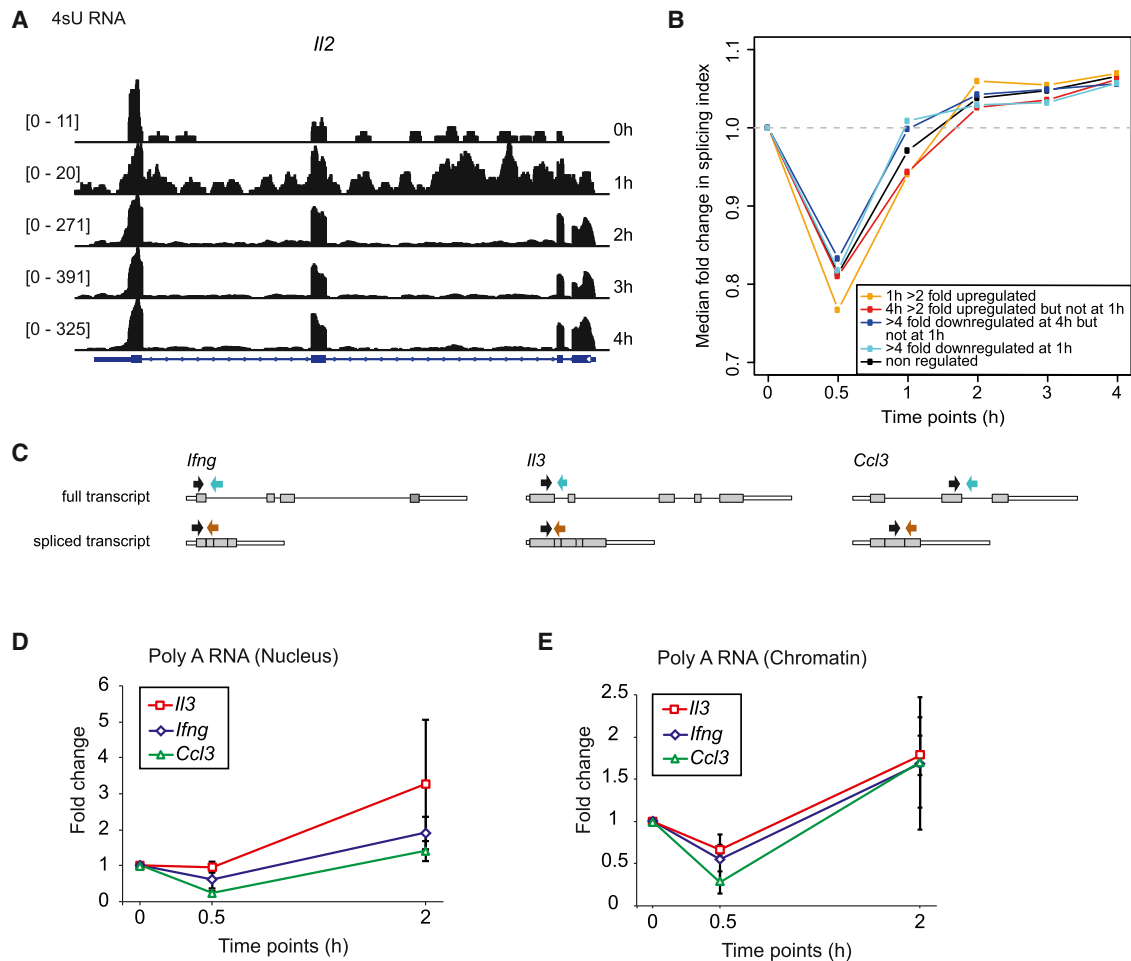


Figure 4. Global Reduction in Cotranscriptional Splicing Rates at the Beginning of Activation

(A) Mapped sequencing reads (4sU RNA) for *Il2*, indicating increased intron read counts 1 hr after activation and reduced intron read counts at later time points. For each time point, the range of read counts (y axis) is indicated in brackets. Gene annotation is indicated as in Figure 1C.

(B) Median fold changes in splicing indices (see Experimental Procedures) over time are displayed for genes upregulated early (≥ 2 -fold upregulated at 1 hr; orange) and at later time points (≥ 2 -fold upregulated at 4 hr, but not at 1 hr; red), genes downregulated early (≥ 4 -fold downregulated at 1 hr; cyan) and at later time points (≥ 4 -fold downregulated at 4 hr, but not 1 hr; blue), and non-regulated genes (fold change < 2 after 4 hr; black).

(C) Schematic overview of primer design to study spliced and unspliced transcripts.

(D and E) Fold changes in the exon/intron ratio determined by qRT-PCR analysis for the polyadenylated whole nucleic fraction (D) and the polyadenylated chromatin fraction (E) for *Il3*, *Ifng*, and *Ccl3*. The mean and SD (error bars) are shown for three (D) or five (E) independent experiments.

show evidence for independent posttranscriptional or translational regulation. Upregulation of genes is mostly mediated by rapid de novo recruitment of RNA Pol II to gene loci, while release of paused RNA Pol II plays only a minor role. This coincides with fluctuations in cotranscriptional splicing rates, which lag at first but are later optimized, as well as a progressive shift toward Ser-2 phosphorylation and activation of pTEFb.

Although previous studies suggested an important role for posttranscriptional mechanisms in the regulation of cytokines during T cell effector activation (Chang et al., 2013; Scheu et al., 2006), it remains controversial to what extent posttranscriptional regulation affects protein expression in general (Larson et al., 2013; Vogel and Marcotte, 2012) or immune cells specifically (Anderson, 2008; Piccirillo et al., 2014). Most of these studies were performed either under steady-state conditions or

in cell lines, and few dynamic studies were performed in immune cells (Bhatt et al., 2012; Jovanovic et al., 2015). The combination of the resulting models nevertheless suggests that changes in mRNA abundance dictate changes in functional properties of the activated immune cell and are thus in line with our findings. This raises the question of whether translational regulation has a greater impact after the actual response or in steady-state conditions. In favor of such a hypothesis are observations from a global study demonstrating that a variety of mRNAs have longer 3' UTRs in resting than in proliferating cells, allowing more posttranscriptional regulation (Sandberg et al., 2008). The independently, posttranscriptionally regulated genes identified in our study tended to have longer 3' UTRs (data not shown). In addition, studies highlighted auto-regulatory feedback loops of posttranscriptional regulators in immune cells. For example,

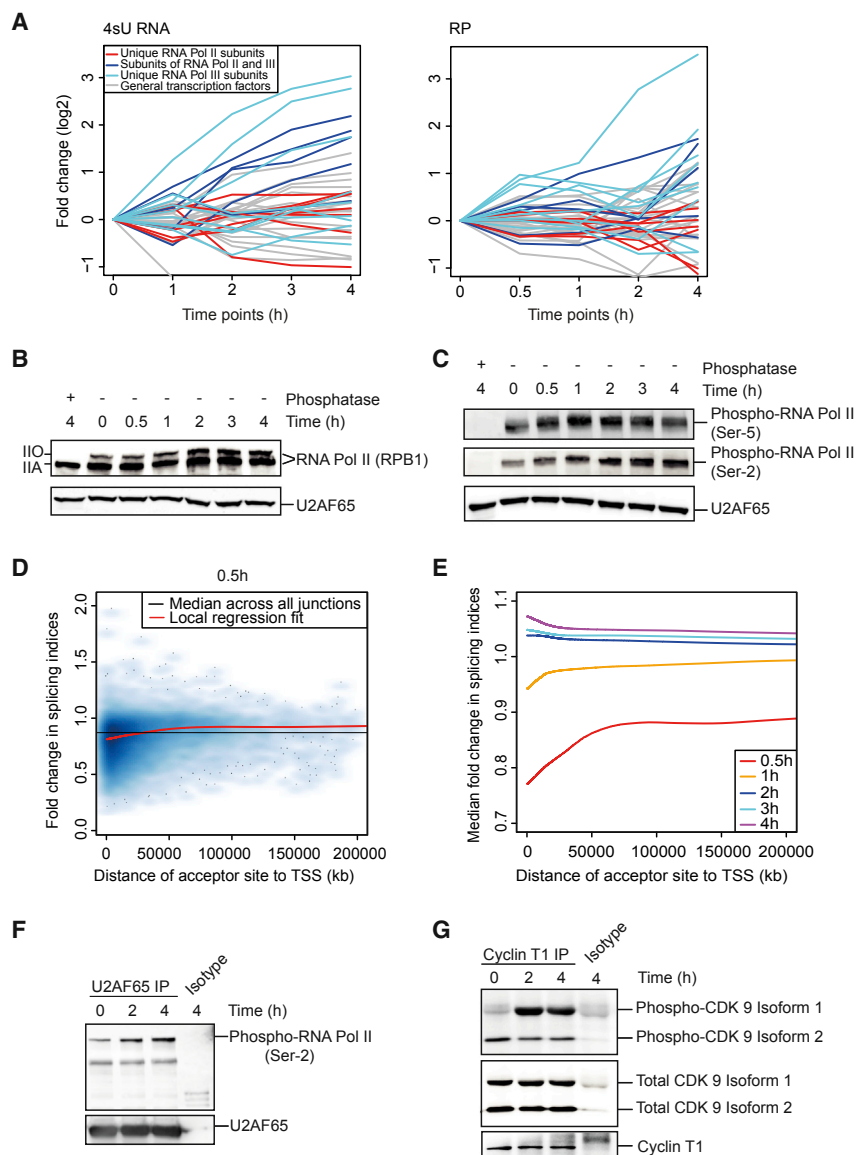


Figure 5. Global Changes in Splicing Rates Correlate with Phosphorylation States of RNA Pol II

(A) Log₂ fold changes over time in 4sU RNA and translated RNA (RP) are shown for genes encoding subunits of RNA Pol II and III and general transcription factors.

(B and C) Western blot analysis of RNA Pol II expression using an antibody against RPB1 (IIO indicates hyper-phosphorylation and activation) (B) and Ser-5 and Ser-2 phosphorylation-specific antibodies (C). U2AF65 was used as loading control.

(D) Fold changes in splicing indices for individual introns at 0.5 hr plotted against the distance of the acceptor site of the intron to the TSS (red line, local regression fit using LOWESS; black line, median).

(E) The local regression fit for intron splicing indices relative to the distance to the TSS is shown for all time points.

(F) Immunoprecipitation at different time points with antibodies recognizing U2AF65 to detect RNA Pol II phosphorylated at Ser-2 of the CTD.

(G) Immunoprecipitation with cyclin T1 to detect phosphorylated CDK9 (Thr186), indicating active elongation complex formations, and total CDK9. Two isoforms of CDK9 could be detected.

Regnase-1 and Roquin, which are degraded during the activation process via the proteasome or proteases, are later re-expressed to ensure posttranscriptional regulation after the actual immune response (Iwasaki et al., 2011; Jeltsch et al., 2014).

Although pausing of RNA Pol II at promoter-proximal positions has been suggested frequently as an important mechanism to maintain genes as highly responsive and activated (Core and Lis, 2008; Muse et al., 2007), our data highlight that de novo recruitment of RNA Pol II plays a more important role, particularly for IEGs. Some studies previously analyzed the processes for IEG induction in primary immune cell responses, specifically for the activation of macrophages and B cells (Fowler et al., 2015; Hargreaves et al., 2009; Kouzine et al., 2013; Ramirez-Carrozzi et al., 2009), as well as global changes in expression during B cell maturation (Kleiman et al., 2015). After activation of bone marrow-derived macrophages and B cells by lipopolysaccha-

rides, release of paused RNA Pol II is the major mechanism driving gene regulation (Fowler et al., 2015; Hargreaves et al., 2009). However, after activation via the B cell receptor, de novo recruitment of RNA Pol II seems to drive transcriptional upregulation in B cells (Fowler et al., 2015). This is in line with our observations for T cells activated via the T cell receptor (TCR). The potential mechanism facilitating this rapid recruitment in T cells remains unclear. Nevertheless, we identified STAT3/4, RelA, and c-Myc as key transcription factors for the gene expression response. C-Myc regulation of translational genes has previously been shown in other contexts (Fernandez et al., 2003), and STAT and Rel proteins are known to control immunological genes in T cell and other immune cell differentiation programs (Coffer et al., 2000; Li et al., 2014; Oeckinghaus and Ghosh, 2009). Therefore, both transcription factor families are likely also acting in the actual T cell effector response, not only during differentiation.

Although it has become evident over the last few years that most mRNAs are cotranscriptionally spliced (Bentley, 2014), little is known how these processes are regulated upon signaling events in mammalian cells (Jonkers and Lis, 2015; Shin and Manley, 2004). In primary macrophages, fluctuations in splicing rates have been observed, both before activation (Hargreaves et al., 2009) and after activation (Bhatt et al., 2012). Some of these observations even led to speculations that they might challenge the concept of cotranscriptional splicing (Sen and Fugmann, 2012; Stower, 2012). In macrophages and T cells, splicing

rates are gradually optimized at later time points, which we correlated with a progressive shift from Ser-5 to Ser-2 phosphorylation of the CTD and activation of CDK9 within the pTEFb complex. Although causality cannot be conclusively shown without better spatial and temporal resolution of RNA Pol II phosphorylation, it is tempting to speculate that massive de novo recruitment of RNA Pol II results in a relative increase of Ser-5 phosphorylation at the beginning of activation that later gradually shifts toward more Ser-2 phosphorylation, enabling efficient splicing. It remains an open question as to how this rapid de novo recruitment is accomplished and whether the temporary reduction in cotranscriptional splicing represents a side effect or an important mechanism at the beginning of cell activation.

EXPERIMENTAL PROCEDURES

Mice

Balb/c DO11.10 TCR transgenic mice and C57BL/6J were purchased from Jackson Laboratory and bred in a specific pathogen-free barrier facility. Mice were euthanized with CO₂ at 8–12 weeks of age for spleen and lymph node removal. All in accordance with the *Helmholtz Zentrum München* institutional as well as the state and federal guidelines.

CD4 T Cell Isolation and Differentiation

Peripheral naive CD4⁺ T cells were isolated and differentiated for 36–48 hr under Th1 conditions. After expansion for additional 2 or 3 days, Th1 cells were activated with anti-CD3 and anti-CD28. For detailed information, see additional [Supplemental Experimental Procedures](#).

Flow Cytometry and Intracellular Cytokine Staining

For intracellular cytokine staining, cells were activated, fixed in 4% paraformaldehyde (PFA) (10 min, room temperature [RT]), permeabilized, and stained with antibodies against IFN γ (eBioscience, 17-7311-82). Representative plots from flow cytometry were all recorded with FACS Aria III (BD Bioscience) and gated on live cells.

qRT-PCR, Western Blotting, and Immunoprecipitation

Total RNA was isolated with QIAzol Lysis Reagent (QIAGEN), and cDNA was synthesized with the QuantiTect Reverse Transcription Kit (QIAGEN, 205311). All quantitative qRT-PCRs were performed with the SYBR green method. The expression levels of *lfn*g mRNA were normalized to the expression of HPRT.

For western blots and immunoprecipitation, cells were lysed in RIPA and Meister lysis buffer, respectively. Total protein concentration was determined according to the bicinchoninic acid assay (BCA) method (Thermo Scientific Pierce). Detailed information is provided in [Supplemental Experimental Procedures](#).

Toxicity Test of 4sU

Cells were treated with different concentrations of 4sU for indicated time points and BH31-1 (500 ng/ μ L) (Sigma, B8809) for 1 hr, or heat shock for 5 min at 95°C was used to induce apoptosis. Apoptotic cells were determined by annexin V/7-aminocoumarinylactinomycin D (7-AAD) (eBioscience, 00-6992) staining and analyzed by flow cytometry. Nuclear stress was determined by p53 accumulation, cytoplasmic stress was determined by eukaryotic translation initiation factor 2a (EIF2a) phosphorylation, and thapsigargin (0.5 μ M) (Sigma, T9033) was used as positive control.

GFP Spike-in Assay

The GFP control plasmid of the Mouse T Cell Nucleofector Kit (Lonza, Cat. No. V4XP-3032) was transfected into expanding Th1 cells 12–15 hr after differentiation according to the manufacturer's instructions. The cells were activated and RNA was taken at indicated time points for qRT-PCR, as described earlier. Genes of interest were normalized to GFP expression.

Subcellular Fractionation and RNA Isolation

Activated Th1 cells were lysed in cytoplasmic lysis buffer, and intact nuclei were isolated with sucrose buffer. The nuclear pellet was resuspended in glycerol buffer, and nuclei lysis buffer was added. After centrifugation, 50 μ L of cold PBS was added to the remaining chromatin pellet and vortexed. Chromatin-associated RNA was extracted by phenol/chloroform extraction and purified according to the QIAGEN RNA cleanup (74204) protocol.

For nuclear RNA, the nuclear pellet was resuspended in 1 mL of lysis/binding buffer, and isolation of polyadenylated RNA was done according to the manufacturer's instructions (μ MACS mRNA isolation kit, Miltenyi Biotec).

cDNA was synthesized with random hexamer and/or oligodeoxythymidylic acid [oligo-d(T)] primers. For detailed information, see additional [Supplemental Experimental Procedures](#).

4sU Labeling, 4sU-Seq, and RP

Samples for RP were prepared according to the manufacturer's instructions (TruSeq Ribo Profile, mammalian; Illumina) with minor changes. Metabolic labeling of newly transcribed RNA with 4sU (Carbosynth, NT0618690), RNA isolation, and biotinylation were performed as described previously ([Rädle et al., 2013](#)) with minor changes. For both total and 4sU RNA samples, library preparation and rRNA depletion were performed using the TruSeq Stranded Total RNA Library Prep Kit (Illumina).

Barcoded libraries were sequenced on a HiSeq 2500 (Illumina) with paired-end, 100 bp reads. Quantification of rRNA depleted 4sU RNA was performed with a Qubit 2.0 Fluorometer. For rRNA depletion, we used the Ribo-Zero Gold rRNA Removal Kit (human, mouse, or rat; Illumina) according to the manufacturer's instructions. Detailed information is provided in [Supplemental Experimental Procedures](#).

ChIP-Seq

Chromatin immunoprecipitation (ChIP) assays were performed as described ([DeKoter et al., 2002](#)) with minor changes. DNA purification was done according to [Blecher-Gonen et al. \(2013\)](#). For further information, see [Supplemental Experimental Procedures](#).

Library preparation was performed from 2 ng of ChIP DNA using the Kapa Hyper Prep Kit with PCR library amplification (KapaBiosystems, KK8504) according to the manufacturer's protocol. The libraries were sequenced on HiSeq 4000, yielding 40–60 million paired reads.

Bioinformatics and Statistical Analysis

RNA-seq and RP reads were mapped against the mm10 mouse reference genome using ContextMap v.2.5.2 ([Bonfert et al., 2015](#)), and ChIP-seq reads were mapped using BWA-MEM v.0.7.13 ([Li and Durbin, 2009](#)). Gene expression and RNA Pol II and H3K36me3 abundance were quantified as FPKM. RNA-seq and RP FPKM values were normalized by median fold changes of ~3,400 housekeeping genes ([Eisenberg and Levanon, 2013](#)). ChIP-seq peaks over input were called with MACS2 v.2.1.0 ([Zhang et al., 2008](#)), with a false discovery rate (FDR) threshold of 0.05. Hierarchical clustering and correlation analysis were performed in R. Translation rates were calculated as RP FPKM to total RNA FPKM. RNA turnover rates were calculated as the 4sU RNA/total RNA ratio in non-activated T cells and normalized to a median RNA half-life of 5 hr. Splicing rates were calculated as splicing index = No. of exon-exon junction reads / (No. of exon-exon junction reads + No. of exon-intron junction reads). Functional and transcription factor target enrichment analysis were performed with Database for Annotation, Visualization and Integrated Discovery (DAVID) ([Huang et al., 2009](#)) and EnrichR ([Chen et al., 2013](#)), respectively. More details can be found in [Supplemental Experimental Procedures](#).

ACCESSION NUMBERS

The accession numbers for the 4sU-seq and total RNA-seq, as well as RP, and for the ChIP-seq data reported in this paper are GEO: GSE83351 and GSE94698. The accession number for the FACS files reported in this paper is FlowRepository: FR-FCM-ZY3V.

SUPPLEMENTAL INFORMATION

Supplemental Information includes Supplemental Experimental Procedures, five figures, and five tables and can be found with this article online at <http://dx.doi.org/10.1016/j.celrep.2017.03.069>.

AUTHOR CONTRIBUTIONS

K.D. and J.L. performed all experiments. C.G. established stress readouts of 4sU. F.G., N.H.U., and K.D. performed ChIP-seq experiments and mapping. C.C.F. analyzed all data with the exception of promoter analysis for transcription factors, which was carried out by M.H. E.G. designed and supervised the project. C.C.F. and E.G. interpreted all results and wrote the manuscript.

ACKNOWLEDGMENTS

We thank Dirk Eick, Harinder Singh, and Shalini Oberdoerffer for critically reviewing the data and/or manuscript; Christine Wolf for some western blot analysis and troubleshooting; Lars Dölken for advice to establish 4sU labeling for primary T cells; Elisabeth Graf and Thomas Schwarzmayr for critical help in library generations and sequencing; Dirk Eick and Andrew Flatley for providing RNA Pol II and T cell antibodies; Matthias von Gamm for mouse colony maintenance; and Annalisa Schaub for proofreading. C.C.F. was supported by grants FR2938/7-1 and CRC 1123 (Z2) from the Deutsche Forschungsgemeinschaft (DFG), and E.G. was supported by the grant GL 870/1-1 from the Deutsche Forschungsgemeinschaft (DFG) and the German Center for Diabetes Research (DZD), Helmholtz Zentrum München.

Received: November 22, 2016

Revised: February 17, 2017

Accepted: March 22, 2017

Published: April 18, 2017

REFERENCES

- Agarwal, S., and Rao, A. (1998). Modulation of chromatin structure regulates cytokine gene expression during T cell differentiation. *Immunity* **9**, 765–775.
- Anderson, P. (2008). Post-transcriptional control of cytokine production. *Nat. Immunol.* **9**, 353–359.
- Ansel, K.M. (2013). RNA regulation of the immune system. *Immunol. Rev.* **253**, 5–11.
- Asano, Y., Shigeta, M., Fathman, C.G., Singer, A., and Hodes, R.J. (1982). Role of the major histocompatibility complex in T cell activation of B cell subpopulations. A single monoclonal T helper cell population activates different B cell subpopulations by distinct pathways. *J. Exp. Med.* **156**, 350–360.
- Baumli, S., Lolli, G., Lowe, E.D., Troiani, S., Rusconi, L., Bullock, A.N., Debreczeni, J.E., Knapp, S., and Johnson, L.N. (2008). The structure of P-TEFb (CDK9/cyclin T1), its complex with flavopiridol and regulation by phosphorylation. *EMBO J.* **27**, 1907–1918.
- Bentley, D.L. (2014). Coupling mRNA processing with transcription in time and space. *Nat. Rev. Genet.* **15**, 163–175.
- Bhatt, D.M., Pandya-Jones, A., Tong, A.J., Barozzi, I., Lissner, M.M., Natoli, G., Black, D.L., and Smale, S.T. (2012). Transcript dynamics of proinflammatory genes revealed by sequence analysis of subcellular RNA fractions. *Cell* **150**, 279–290.
- Blecher-Gonen, R., Barnett-Iltzhaki, Z., Jaitin, D., Amann-Zalcenstein, D., Lara-Astiaso, D., and Amit, I. (2013). High-throughput chromatin immunoprecipitation for genome-wide mapping of in vivo protein-DNA interactions and epigenomic states. *Nat. Protoc.* **8**, 539–554.
- Bonfert, T., Kirner, E., Csaba, G., Zimmer, R., and Friedel, C.C. (2015). ContextMap 2: fast and accurate context-based RNA-seq mapping. *BMC Bioinformatics* **16**, 122.
- Burger, K., Mühl, B., Kellner, M., Rohmoser, M., Gruber-Eber, A., Windhager, L., Friedel, C.C., Dölken, L., and Eick, D. (2013). Rridine inhibits rRNA synthesis and causes a nucleolar stress response. *RNA Biol.* **10**, 1623–1630.
- Carpenter, S., Ricci, E.P., Mercier, B.C., Moore, M.J., and Fitzgerald, K.A. (2014). Post-transcriptional regulation of gene expression in innate immunity. *Nat. Rev. Immunol.* **14**, 361–376.
- Chang, C.H., Curtis, J.D., Maggi, L.B., Jr., Faubert, B., Villarino, A.V., O'Sullivan, D., Huang, S.C., van der Windt, G.J., Blagih, J., Qiu, J., et al. (2013). Posttranscriptional control of T cell effector function by aerobic glycolysis. *Cell* **153**, 1239–1251.
- Chen, E.Y., Tan, C.M., Kou, Y., Duan, Q., Wang, Z., Meirelles, G.V., Clark, N.R., and Ma'ayan, A. (2013). Enrichr: interactive and collaborative HTML5 gene list enrichment analysis tool. *BMC Bioinformatics* **14**, 128.
- Chou, C., Pinto, A.K., Curtis, J.D., Persaud, S.P., Cella, M., Lin, C.C., Edelson, B.T., Allen, P.M., Colonna, M., Pearce, E.L., et al. (2014). c-Myc-induced transcription factor AP4 is required for host protection mediated by CD8+ T cells. *Nat. Immunol.* **15**, 884–893.
- Coffer, P.J., Koenderman, L., and de Groot, R.P. (2000). The role of STATs in myeloid differentiation and leukemia. *Oncogene* **19**, 2511–2522.
- Core, L.J., and Lis, J.T. (2008). Transcription regulation through promoter-proximal pausing of RNA polymerase II. *Science* **319**, 1791–1792.
- Core, L.J., Waterfall, J.J., and Lis, J.T. (2008). Nascent RNA sequencing reveals widespread pausing and divergent initiation at human promoters. *Science* **322**, 1845–1848.
- DeKoter, R.P., Lee, H.J., and Singh, H. (2002). PU.1 regulates expression of the interleukin-7 receptor in lymphoid progenitors. *Immunity* **16**, 297–309.
- Eichelbaum, K., and Krijgsvelde, J. (2014). Rapid temporal dynamics of transcription, protein synthesis, and secretion during macrophage activation. *Mol. Cell. Proteomics* **13**, 792–810.
- Eisenberg, E., and Levanon, E.Y. (2013). Human housekeeping genes, revisited. *Trends Genet.* **29**, 569–574.
- Fernandez, P.C., Frank, S.R., Wang, L., Schroeder, M., Liu, S., Greene, J., Cocito, A., and Amati, B. (2003). Genomic targets of the human c-Myc protein. *Genes Dev.* **17**, 1115–1129.
- Fowler, T., Garruss, A.S., Ghosh, A., De, S., Becker, K.G., Wood, W.H., Weirauch, M.T., Smale, S.T., Aronow, B., Sen, R., and Roy, A.L. (2015). Divergence of transcriptional landscape occurs early in B cell activation. *Epigenetics Chromatin* **8**, 20.
- Friedel, C.C., Dölken, L., Ruzsics, Z., Koszinowski, U.H., and Zimmer, R. (2009). Conserved principles of mammalian transcriptional regulation revealed by RNA half-life. *Nucleic Acids Res.* **37**, e115.
- Hamilton, K.S., Phong, B., Corey, C., Cheng, J., Gorentla, B., Zhong, X., Shiva, S., and Kane, L.P. (2014). T cell receptor-dependent activation of mTOR signaling in T cells is mediated by Carma1 and MALT1, but not Bcl10. *Sci. Signal.* **7**, ra55.
- Haque, N., and Oberdoerffer, S. (2014). Chromatin and splicing. *Methods Mol. Biol.* **1126**, 97–113.
- Hargreaves, D.C., Horng, T., and Medzhitov, R. (2009). Control of inducible gene expression by signal-dependent transcriptional elongation. *Cell* **138**, 129–145.
- Huang, D.W., Sherman, B.T., and Lempicki, R.A. (2009). Systematic and integrative analysis of large gene lists using DAVID bioinformatics resources. *Nat. Protoc.* **4**, 44–57.
- Ingolia, N.T., Brar, G.A., Rouskin, S., McGeachy, A.M., and Weissman, J.S. (2012). The ribosome profiling strategy for monitoring translation in vivo by deep sequencing of ribosome-protected mRNA fragments. *Nat. Protoc.* **7**, 1534–1550.
- Iwasaki, H., Takeuchi, O., Teraguchi, S., Matsushita, K., Uehata, T., Kuniyoshi, K., Satoh, T., Saitoh, T., Matsushita, M., Standley, D.M., and Akira, S. (2011). The I κ B kinase complex regulates the stability of cytokine-encoding mRNA induced by TLR-IL-1R by controlling degradation of regnase-1. *Nat. Immunol.* **12**, 1167–1175.
- Jeltsch, K.M., Hu, D., Brenner, S., Zöller, J., Heinz, G.A., Nagel, D., Vogel, K.U., Rehage, N., Warth, S.C., Edelmann, S.L., et al. (2014). Cleavage of roiquin and regnase-1 by the paracaspase MALT1 releases their cooperatively repressed targets to promote T(H)17 differentiation. *Nat. Immunol.* **15**, 1079–1089.

- Jonkers, I., and Lis, J.T. (2015). Getting up to speed with transcription elongation by RNA polymerase II. *Nat. Rev. Mol. Cell Biol.* *16*, 167–177.
- Jovanovic, M., Rooney, M.S., Mertins, P., Przybylski, D., Chevrier, N., Satija, R., Rodriguez, E.H., Fields, A.P., Schwartz, S., Raychowdhury, R., et al. (2015). Immunogenetics. Dynamic profiling of the protein life cycle in response to pathogens. *Science* *347*, 1259038.
- Kedersha, N.L., Gupta, M., Li, W., Miller, I., and Anderson, P. (1999). RNA-binding proteins TIA-1 and TIAR link the phosphorylation of eIF-2 alpha to the assembly of mammalian stress granules. *J. Cell Biol.* *147*, 1431–1442.
- Kleiman, E., Salyakina, D., De Heusch, M., Hoek, K.L., Llanes, J.M., Castro, I., Wright, J.A., Clark, E.S., Dykxhoorn, D.M., Capobianco, E., et al. (2015). Distinct transcriptomic features are associated with transitional and mature B-cell populations in the mouse spleen. *Front. Immunol.* *6*, 30.
- Komarnitsky, P., Cho, E.J., and Buratowski, S. (2000). Different phosphorylated forms of RNA polymerase II and associated mRNA processing factors during transcription. *Genes Dev.* *14*, 2452–2460.
- Kouzine, F., Wojtowicz, D., Yamane, A., Resch, W., Kieffer-Kwon, K.R., Bandle, R., Nelson, S., Nakahashi, H., Awasthi, P., Feigenbaum, L., et al. (2013). Global regulation of promoter melting in naive lymphocytes. *Cell* *153*, 988–999.
- Larsson, O., Tian, B., and Sonenberg, N. (2013). Toward a genome-wide landscape of translational control. *Cold Spring Harb. Perspect. Biol.* *5*, a012302.
- Li, H., and Durbin, R. (2009). Fast and accurate short read alignment with Burrows-Wheeler transform. *Bioinformatics* *25*, 1754–1760.
- Li, P., Spolski, R., Liao, W., and Leonard, W.J. (2014). Complex interactions of transcription factors in mediating cytokine biology in T cells. *Immunol. Rev.* *261*, 141–156.
- Listerman, I., Sapra, A.K., and Neugebauer, K.M. (2006). Cotranscriptional coupling of splicing factor recruitment and precursor messenger RNA splicing in mammalian cells. *Nat. Struct. Mol. Biol.* *13*, 815–822.
- Murphy, K.M., and Reiner, S.L. (2002). The lineage decisions of helper T cells. *Nat. Rev. Immunol.* *2*, 933–944.
- Muse, G.W., Gilchrist, D.A., Nechaev, S., Shah, R., Parker, J.S., Grissom, S.F., Zeitlinger, J., and Adelman, K. (2007). RNA polymerase is poised for activation across the genome. *Nat. Genet.* *39*, 1507–1511.
- O’Shea, J. (2015). A first look at TH cell transcriptomes. *Nat. Rev. Immunol.* *15*, 668.
- Oeckinghaus, A., and Ghosh, S. (2009). The NF-kappaB family of transcription factors and its regulation. *Cold Spring Harb. Perspect. Biol.* *1*, a000034.
- Phatnani, H.P., and Greenleaf, A.L. (2006). Phosphorylation and functions of the RNA polymerase II CTD. *Genes Dev.* *20*, 2922–2936.
- Piccirillo, C.A., Bjur, E., Topisirovic, I., Sonenberg, N., and Larsson, O. (2014). Translational control of immune responses: from transcripts to translomes. *Nat. Immunol.* *15*, 503–511.
- Rädle, B., Rutkowski, A.J., Ruzsics, Z., Friedel, C.C., Koszinowski, U.H., and Dölken, L. (2013). Metabolic labeling of newly transcribed RNA for high resolution gene expression profiling of RNA synthesis, processing and decay in cell culture. *J. Vis. Exp.* (78), 50195.
- Ramirez-Carrozzi, V.R., Braas, D., Bhatt, D.M., Cheng, C.S., Hong, C., Doty, K.R., Black, J.C., Hoffmann, A., Carey, M., and Smale, S.T. (2009). A unifying model for the selective regulation of inducible transcription by CpG islands and nucleosome remodeling. *Cell* *138*, 114–128.
- Rutkowski, A.J., Erhard, F., L’Hernault, A., Bonfert, T., Schilhabel, M., Crump, C., Rosenstiel, P., Efstathiou, S., Zimmer, R., Friedel, C.C., and Dölken, L. (2015). Widespread disruption of host transcription termination in HSV-1 infection. *Nat. Commun.* *6*, 7126.
- Sandberg, R., Neilson, J.R., Sarma, A., Sharp, P.A., and Burge, C.B. (2008). Proliferating cells express mRNAs with shortened 3’ untranslated regions and fewer microRNA target sites. *Science* *320*, 1643–1647.
- Scheu, S., Stetson, D.B., Reinhardt, R.L., Leber, J.H., Mohrs, M., and Locksley, R.M. (2006). Activation of the integrated stress response during T helper cell differentiation. *Nat. Immunol.* *7*, 644–651.
- Schüller, R., Forné, I., Straub, T., Schrieck, A., Texier, Y., Shah, N., Decker, T.M., Cramer, P., Imhof, A., and Eick, D. (2016). Heptad-specific phosphorylation of RNA polymerase II CTD. *Mol. Cell* *61*, 305–314.
- Schwartz, S., Meshorer, E., and Ast, G. (2009). Chromatin organization marks exon-intron structure. *Nat. Struct. Mol. Biol.* *16*, 990–995.
- Sen, R., and Fugmann, S.D. (2012). Transcription, splicing, and release: are we there yet? *Cell* *150*, 241–243.
- Shin, C., and Manley, J.L. (2004). Cell signalling and the control of pre-mRNA splicing. *Nat. Rev. Mol. Cell Biol.* *5*, 727–738.
- Singh, H. (2014). Transcriptional and epigenetic networks orchestrating immune cell development and function. *Immunol. Rev.* *261*, 5–8.
- Smale, S.T. (2014). Transcriptional regulation in the immune system: a status report. *Trends Immunol.* *35*, 190–194.
- Stower, H. (2012). Splicing: waiting to be spliced. *Nat. Rev. Genet.* *13*, 599.
- Szabo, S.J., Sullivan, B.M., Peng, S.L., and Glimcher, L.H. (2003). Molecular mechanisms regulating Th1 immune responses. *Annu. Rev. Immunol.* *21*, 713–758.
- Venkatesh, S., and Workman, J.L. (2013). Set2 mediated H3 lysine 36 methylation: regulation of transcription elongation and implications in organismal development. *Wiley Interdiscip. Rev. Dev. Biol.* *2*, 685–700.
- Vogel, C., and Marcotte, E.M. (2012). Insights into the regulation of protein abundance from proteomic and transcriptomic analyses. *Nat. Rev. Genet.* *13*, 227–232.
- Wang, C., Collins, M., and Kuchroo, V.K. (2015). Effector T cell differentiation: are master regulators of effector T cells still the masters? *Curr. Opin. Immunol.* *37*, 6–10.
- Windhager, L., Bonfert, T., Burger, K., Ruzsics, Z., Krebs, S., Kaufmann, S., Malterer, G., L’Hernault, A., Schilhabel, M., Schreiber, S., et al. (2012). Ultra-short and progressive 4sU-tagging reveals key characteristics of RNA processing at nucleotide resolution. *Genome Res.* *22*, 2031–2042.
- Zhang, Y., Liu, T., Meyer, C.A., Eeckhoute, J., Johnson, D.S., Bernstein, B.E., Nusbaum, C., Myers, R.M., Brown, M., Li, W., and Liu, X.S. (2008). Model-based analysis of ChIP-seq (MACS). *Genome Biol.* *9*, R137.
- Zhu, J., Yamane, H., and Paul, W.E. (2010). Differentiation of effector CD4 T cell populations (*). *Annu. Rev. Immunol.* *28*, 445–489.